

CONFORMAL COATING - RELATIVE PERFORMANCE COMPARISON THROUGH ENVIRONMENTAL TESTING USING IPC B-52 TEST BOARD

Domingo Vazquez, Alfredo Garcia, Ricardo Macias, Humberto Ramirez,
Cristina Amador, Iulia Muntele, Shane Lewis, Mulugeta Abteu
Sanmina Corporation
iulia.muntele@sanmina.com

Jeff Chinn
Integrated Surface Technologies, Inc.
info@insurftech.com

ABSTRACT

Conformal coating - partial or full application using immersion, spray, vapor deposition or other methods, as the coating material formulation requires, has as ultimate goal protection of the assembled board or specific components from the effects of the working environment. Typical environmental testing applied to qualify conformal coating material involves humidity and temperature cycling, and exposure to corrosive environments. The limited scope experiment presented here has the intent to compare the behavior of a typical acrylic coating used on large scale in various applications and of a specific super-hydrophobic nano conformal coating formulation. Review of the fundamental properties of the coating materials place the nano coating in a more favorable position than the typical acrylic coating. Additionally, as an invisible nanometer thick coating that is a dielectric, repels water, adds negligible mass to a printed circuit card, can be applied without masking, does not require removal at rework, and does not impede heat transfer, nano coating could be an attractive alternative to existing conformal coating materials. For practical verification, a batch of IPC B-52 boards were assembled in a no clean lead free process. Subsequent processes steps were applied and once coated, the boards were submitted for environmental exposure and SIR (surface insulation resistance) measurements.

Key words: conformal coating, super-hydrophobicity

INTRODUCTION

Increased and expanded use of complex printed circuit board assembly (PCBA) across the globe in increasingly diverse environments leads to the need to protect these products from the effects of pollution, coastal atmosphere, and moisture ingress. Most coatings act like a porous physical barrier to humidity, allowing it to permeate but preventing it from bridging across circuits; additionally, others act as humidity repellants as well. The conformal coating barrier increases the SIR at board surface, hence reducing the possibility for cross-talk, electrical leakage, corrosion, etc [9]. For different applications, one class of hydrophobic materials involves deposition of nano layers

of silica and alumina [2, 3], while others use titanium oxide or zinc oxide, depending on the intended application [1, 8]. The nano coating chosen for this experiment is textured alumina applied to the sample using the hybrid atomic layer deposition/chemical vapor deposition technique (also called vapor particle deposition). It has the advantage of being water repellent (super-hydrophobic), while also allowing easy rework and not requiring any masking for application. It has been documented elsewhere [2] that a thick coating will affect electrical contact of connectors, while typical nanometer layer thickness has no adverse effect. However, regardless of its thickness, the coating is considered to be mechanically fragile and can be removed in the event the boards are grossly mishandled. An advantage of this type coating is that it does not interact with the eventual flux residue present on the board. It is assumed based on experience with other conformal coating materials that there would be other advantages to cleaning the flux residue before coating. SIR measurements [5] are used on one hand for assessing cleanliness; on the other hand SIR measurements are an indication of the permeability of the coatings to moisture and contaminants and it can also illustrate the relative performance of different coatings [9].

The SIR data obtained in this experiment are a combined result of the effect of the respective test environment on the board surface finish, any process residue acquired through board processing, and conformal coating material properties.

EXPERIMENTAL

IPC-B-52 test board was chosen due to its novelty and versatility. The printed wired board (PWB) was chosen with immersion silver finish due to its widespread use, and all the components in the board kit were populated on the board in a no-clean, lead free assembly process with a maximum peak temperature of 250 °C. All components were assembled in surface mount (SMT) process, using intrusive reflow for through hole parts. The boards were inspected and found to be defect free using X-ray inspection and electrical continuity measurements. A

summary of the design of experiment (DOE) run is included in the Table 1.

Table 1: Test board experiment conditions.

Run #	Wash condition	Coating type	No. of boards	Board label	Plasma cleaning
1	No	Nano coating	12	RN1 through RN12	RN1, RN2 RN5, RN6 RN9, RN10
2	Yes	Nano coating	12	RY1 through RY12	
3	Yes	Acrylic	12	AY1 through AY12	
4	No	Acrylic	12	AN1 Through AN12	AN1, AN2 AN5, AN6 AN9, AN10
5	No	Nano coating	4	RN13 through RN16	RN13, RN14, RN15, RN16
6	Yes	Nano coating	4	RY13 through RY16	

The boards were split in 2 groups after SMT assembly. Half of the boards were sent through an in-line cleaner using an engineering fluid for cleaning no-clean flux residue in an aqueous environment. Steps 5 and 6 were duplicated after a rework step included after the nano coating was initially applied. The 8 boards were recoated with the same material once the rework was completed. Selected boards were subjected to plasma cleaning before coating was applied. Acrylic coating thickness was specified in the range of 3-4 mils. Ion chromatography (IC) coupons were sectioned out of the board and sent for measurement. These coupons were essentially two sets of samples, the difference between them being whether they were washed after SMT assembly or not. Global and local extraction data acquired on selected coupons is shown in the following graphs. The ion chromatography instrument used is Dionex ICS-2100 system. The global extraction was done according to IPC-TM-650 Method 2-3-28b; the calibration of the measurement was done using traceable calibration standard solutions.

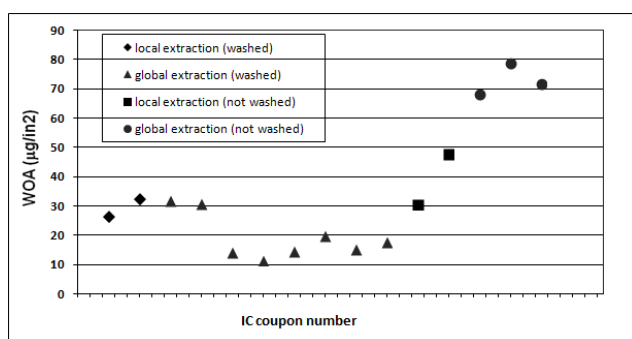


Figure 1: WOA (weak organic acids) level measured for different samples using either local or global extraction methods.

Except for weak organic acids residues (Figure 1) when measured either through local extraction or global extraction on non washed boards, the anion and cation contaminants in the flux residue were found to be in the expected range (Table 2 and Table 3). IPC-9203 [5] advises that is prudent for the user to establish a correlation

Table 1: Measured anions contamination levels.

coupon label	Fluoride	Chloride	Nitrite	Bromide	Nitrate	Sulfate	Phosphate
global extraction (Level ppm (µg/in2))							
RY03	1.0299	0.3362	0.1069	0.0000	0.2395	0.7996	0.0592
RY04	0.9172	0.2991	0.0416	0.0000	0.1875	0.6204	0.0406
RY08	0.8730	0.2940	0.0365	0.0000	0.2127	0.6154	0.0623
RY12	0.8746	0.2782	0.0393	0.0000	0.2536	0.7793	0.1076
AY03	0.9100	0.2616	0.0438	0.0000	0.2055	0.7847	0.0625
AY04	0.8773	0.2538	0.0893	0.0000	0.1897	0.5474	0.0639
AY08	0.9051	0.2487	0.0979	0.0000	0.2772	0.9967	0.0723
AY12	0.9752	0.3063	0.0729	0.0000	0.2397	0.6740	0.0654
AN03	1.0826	1.1368	0.0000	0.0000	0.4989	1.7715	0.2227
AN07	1.1645	1.3124	0.0000	0.0000	0.3589	1.6970	0.0918
AN11	1.1319	1.0004	0.1438	0.0000	0.3387	1.3913	1.0389
local extraction (Level ppm (µg/in2))							
AN01	1.2145	1.3930	0.2170	0.0000	0.6825	2.3940	0.0000
AN02	1.2696	2.1043	0.2210	0.0000	1.4835	2.0903	0.0000
RY01	1.2733	1.4101	0.3262	0.0000	0.7086	2.2555	0.0000
RY02	1.2788	1.6432	0.2768	0.0000	0.8969	2.1407	0.0000
Max limits	3	4	3	10	3	3	3

Table 2: Measured cation contamination levels.

coupon label	Lithium	Sodium	Ammonium	Potassium	Magnesium	Calcium
global extraction (Level ppm (µg/in2))						
RY03		0.7068	0.4358	0.4102	0.0348	0.5788
RY04		0.6134	0.4116	0.3323	0.0217	0.4999
RY08		0.5179	0.4604	0.2602	0.0303	0.5179
RY12		0.5323	0.4147	0.3087	0.0361	0.4278
AY03		0.6144	0.5019	0.2415	0.0383	0.4868
AY04		0.5677	0.3907	0.3831	0.0379	0.3839
AY08		0.5036	0.3843	0.2938	0.0334	0.4585
AY12		0.7105	0.4308	0.3257	0.0373	0.4640
AN03		1.0408	0.4407	0.4384	0.0656	0.9178
AN07	0.004507	1.2913	0.4054	0.4677	0.0621	0.7988
AN11		1.0791	0.4069	0.4993	0.0500	0.9117
local extraction (Level ppm (µg/in2))						
AN01	0	0.8785	0.0000	0.0000	0.0000	0.2170
AN02	0	1.3538	0.0000	0.7260	0.0000	1.1574
RY01	0	0.7927	0.0000	0.5086	0.0000	1.4908
RY02	0	1.2052	0.0000	1.1877	0.0000	1.6607
Max limits	3	3	3	3	1	1

between the IC and SIR measurements. Based on the selected coupons used for IC measurement, it was observed that low levels of WOA correspond with high SIR readings only for the temperature/humidity/bias (THB) test. For the corrosive gas test and the salt spray test, the high or low readings of WOA did not correlate with the observed SIR values.

C3 electrical testing was done for all local extractions. All samples passed the 250/120 corrosivity index condition [4], except for coupon labeled AN01. This coupon did not go through the wash sequence after SMT assembly; however, the IC measurement of the extracted solution did not differ from the rest of the coupons.

Nano conformal coating material. While the acrylic coating is a well known entity, the nano conformal coating requires further discussion. The nano coating application process has a significant impact on the coating structure. The nano coating is applied using a technology called Vapor Particle Deposition (VPD), although a textured film can be obtained either through an additive or subtractive method. Using an additive method, along with the metal or semiconductor oxide nano particles, two other materials from the silane family are introduced (either simultaneously with the nano particles or as in this case,

sequentially): a coupling agent, acting as a link/glue between the substrate and the alumina nano particles (obtained from oxidization of an organoaluminium precursor), and a surface energy lowering agent. Four properties may be used to define a suitable textured nano composite film: roughness, coverage, durability and surface energy. The most sought after characteristic of such coating is its ability to repel water. A contact angle higher than 150° characterizes the coating as super-hydrophobic. A dedicated coating chamber allows for rigorous control of critical process parameters, and can deliver up to 5 different precursors to create custom nano-composite films.

Environmental Testing. Three tests were selected to be applied to the coated B-52 SIR coupons based on the following standards: IPC TM-650 method 2.6.3.4A for humidity testing (65% RH, 40°C, 5V DC, 168 hours), BS EN 60068-2-60 Method 1 for corrosive gas testing (mixed gas environment combining hydrogen sulfide and sulfur dioxide), and IEC 60068-2-11 for salt mist testing (5% salt solution, 35°C, 168 hours). Method 2.6.3.4A [6] was modified according to IPC-9203 standard for IPC B-52 test board. The SIR coupons were distributed between the three tests as shown in Table 4. None of the tests included non-coated witness samples due to the scope of the experiment to compare the behavior of the nano coated samples relative to the acrylic coated samples. The acceptance criteria for temperature/humidity/bias (THB) test is given by the IPC-9202 document (Material and Process Characterization/Qualification, Test Protocol for Assessing Electrochemical Performance): “All tested SIR patterns shall show a minimum resistance of 100 megaohms (>10⁸ ohms), beginning 24 hours after the chamber has stabilized at the elevated test condition.” Other standards establish different threshold values. For example, the IPC-CC-830 document suggests a threshold limit of minimum 5 GΩ, while the Telcordia GR - 78 document from 2007 requires 7 GΩ (Section 14.4). For this reason, the graphs contain two threshold limits, one at 9.7 corresponding to log₁₀(5×10⁹), and one at 8 corresponding to log₁₀(100×10⁶).

Table 4: SIR coupons distribution between the three tests. Underlined are the boards which received plasma treatment before coating.

Test 1: Temperature/Humidity/Bias	Test 2: Salt mist	Test 3: Corrosive gas
<u>RN1</u> , RY1, <u>AN1</u> , AY1, <u>RN2</u> , RY2, <u>AN2</u> , AY2, RN3, RY3, AN3, AY3, RN4, RY4, AN4, AY4	<u>RN5</u> , RY5, <u>AN5</u> , AY5, <u>RN6</u> , RY6, <u>AN6</u> , AY6, RN7, RY7, AN7, AY7, RN8, RY8, AN8, AY8	<u>RN9</u> , RY9, <u>AN9</u> , AY9, <u>RN10</u> , RY10, <u>AN10</u> , AY10, RN11, RY11, AN11, AY11, RN12, RY12, AN12, AY12
<u>RN13</u> , <u>RN14</u> , <u>RN15</u> , <u>RN16</u> , RY13, RY14, RY15, RY16		

Some authors [7] consider that the significant data is acquired on the first 24 hours of a SIR test. Resistivity measurements and visual inspection data from the three tests are shown below. Initial SIR readings on all 56 boards regardless of the coating type and surface preparation conditions were above 5 GΩ.

RESULTS AND DISCUSSION

Corrosive Gas Test. Sixteen SIR coupons as labeled in Table 4 were placed in the chamber for mix gas test. The samples surface resistance was measured before test and 24 hours after the test. Non-coated witness samples were not included in this test.

The samples coated with acrylic showed systematically higher surface insulation values both before and after the test. The criteria chosen for test pass are a value of resistance of 5 GΩ or higher. The plots of the measured SIR values include an additional reference line at 100 MΩ.

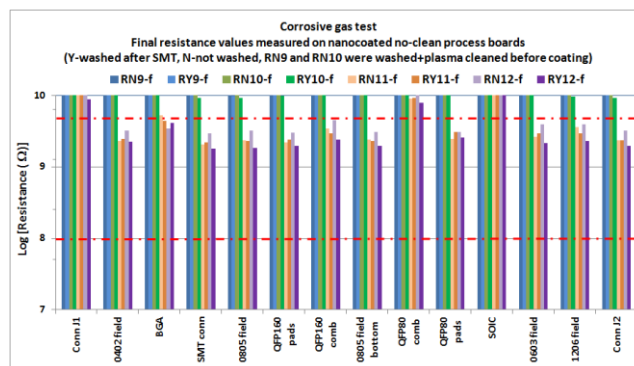


Figure 2: Nanocoated (washed and not washed boards) boards surface insulation resistance values measured after the corrosive gas test. Data is grouped by SIR pattern, each bar represents one board.

An immediate observation based on Figure 2 is that either washing or not washing the no-clean boards after SMT assembly, has a 50/50 outcome when the coating is the super-hydrophobic nano coating: 2 of the washed boards (RY9 and RY10) perform comparably to the plasma treated boards (RN9 and RN10), while two of the washed boards (RY11 and RY12) perform the same as the not washed and non plasma treated boards (RN11 and RN12). The higher surface insulation values after corrosive gas test were shown by the no-washed after SMT boards (RN9 and RN10) which were later washed and plasma treated before nano coating was applied. Among the not washed after SMT assembly, boards RN11 and RN12 show lower than 5 GΩ values after the corrosive gas test. Among the washed after SMT assembly, all boards have initial values higher than 5 GΩ; after the test, two of the boards read above 5 GΩ, and two have values below 5 GΩ. In addition to boards washing, plasma treatment before application of the super-hydrophobic nano coating is a supplier recommended process for obtaining the desired performance of the nano coating, even if the boards are not washed immediately after SMT assembly.

All the acrylic coated boards have shown consistent high surface insulation values both before and after the corrosive gas test, with values readings above 5GΩ – no graph was included. Among the acrylic coated boards, the boards labeled AN9 and AN10 received the wash followed by plasma cleaning before the acrylic coating was applied.

After test, only the acrylic coated boards met and exceeded the high threshold surface insulation resistance value. Figure 3 contains an illustration of the main effects, as data was averaged over all SIR patterns. The dashed line in Figure 3 signifies the 5 GΩ threshold; the data points above the dashed line met the threshold condition 100% (all boards and all SIR patterns associated for the respective surface treatment case). In this test all data is above the 100 MΩ limit.

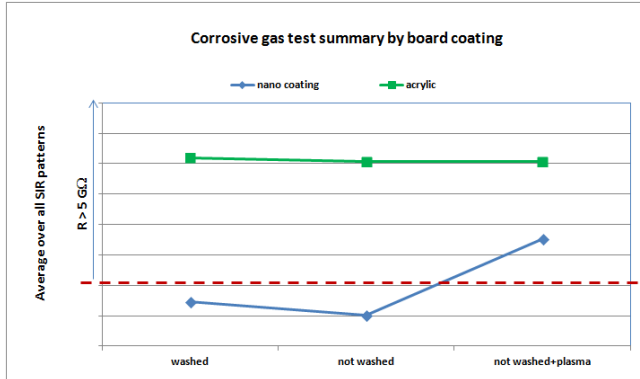


Figure 3. Corrosive gas test: Average ranking over all SIR patterns, irrespective of the geometry, for each surface treatment applied. Threshold limit is 5 GΩ.

2. Salt Spray Test. The test included 16 B-52 boards. All boards measured above 5 GΩ before the test. After the test, one board of each in the washed after SMT batch measured on all SIR patterns above this threshold value. One variable introduced by the salt fog test is the accumulation of salt at the locations where the wires were hand soldered by the lab for measurement purposes, and subsequent brush cleaning done with deionized water and isopropyl alcohol. Included below (Figure 4) are images of the boards as placed in the test chamber and details of the boards after salt spray test.

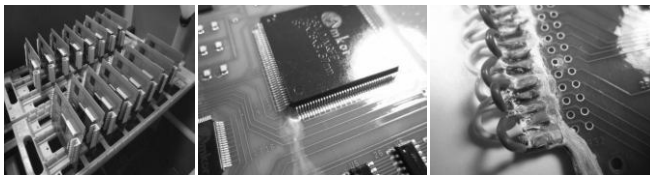


Figure 4. Boards for salt fog test as placed in the test chamber and after the completion of the test.

The compiled SIR data for the nano coated and for the acrylic coated boards is shown in Table 5. For both type coatings, only one board in each batch passed the 5 GΩ threshold condition after test. When checking the final measured surface resistance against the lower acceptance value of 100 MΩ, the not washed nano coated boards are all pass, while half of the SIR patterns on the board labeled

Table 5. SIR values at the end of the salt spray test. The data is given as log10 of the measured resistance (Ω).

SIR pattern/Bord #	Log10 of SIR measurements at the end of salt spray test - nano coating							
	RN5	RN6	RN7	RN8	RY5	RY6	RY7	RY8
Connector J1	9.2	8.7	9.4	9.6	8.6	9.5	10.4	9.9
0402 field	9.7	9.9	9.6	9.7	7.4	9.4	10.2	10.1
BGA	9.0	8.6	8.9	9.3	5.7	9.0	9.5	10.1
SMT connector	8.9	8.9	8.9	9.3	7.0	8.9	9.2	9.9
0805 field	9.2	9.4	9.2	9.6	8.8	9.4	9.9	10.0
QFP160 pads	8.7	8.6	8.9	9.4	5.4	8.9	9.1	9.9
QFP160 comb	8.8	9.7	8.9	9.4	7.9	8.9	9.3	10.1
0805 field bottom	9.8	9.1	10.0	10.0	7.0	9.1	9.7	10.1
QFP80 comb	9.1	9.1	9.3	9.6	8.4	9.2	9.6	10.0
QFP80 pads	8.8	8.7	8.9	9.4	6.6	8.9	9.4	10.0
SOIC	8.7	9.2	9.4	10.0	8.9	9.5	10.3	10.4
0603 field	9.4	9.7	9.5	9.8	8.9	9.4	10.0	10.2
1206 field	9.5	9.6	9.7	9.8	8.5	9.2	10.0	10.1
Connector J2	8.8	8.6	8.9	9.4	6.5	9.0	9.5	10.0

SIR pattern/Bord #	Log10 of SIR measurements at the end of salt spray test - acrylic coating							
	AN5	AN6	AN7	AN8	AY5	AY6	AY7	AY8
Connector J1	6.85	7.73	8.80	8.59	7.66	8.22	11.94	7.70
0402 field	8.88	8.49	9.09	8.83	8.34	8.94	11.59	8.42
BGA	8.45	8.19	8.43	8.64	7.85	7.92	10.02	7.43
SMT connector	7.23	7.54	7.80	7.76	7.90	7.98	9.98	7.23
0805 field	8.70	8.64	8.76	10.07	8.61	8.86	11.39	8.50
QFP160 pads	7.76	7.65	7.95	10.82	7.98	7.28	9.96	7.46
QFP160 comb	8.33	8.00	8.05	7.92	8.27	7.87	9.98	7.62
0805 field bottom	8.83	8.57	8.85	8.45	8.73	9.01	10.76	8.23
QFP80 comb	7.72	8.29	8.68	8.14	8.28	8.03	9.96	7.73
QFP80 pads	8.08	7.82	8.23	8.06	8.14	8.18	9.96	7.83
SOIC	8.66	8.21	8.78	8.78	8.69	8.73	10.52	7.94
0603 field	8.46	8.60	8.70	8.57	8.44	8.70	10.16	8.05
1206 field	9.11	8.67	8.80	8.59	8.48	8.63	10.60	8.27
Connector J2	7.78	7.89	8.15	8.13	8.18	8.27	9.88	7.85

RY5 from the washed nano coated boards batch do not meet this lower threshold value. At the same time, most of the boards coated with acrylic (except for the board labeled AY7) do not meet the lower threshold value on several SIR patterns.

Half of the boards not washed after SMT were applied additional surface treatment at the coating site where these boards were washed and plasma treated.

The salt mist test is overly harsh for both types of coatings. Even so, each coating has presented one board with high SIR values. Additionally, there might have been additional variables inserted at the cleaning step after the test due to the salt deposits accumulated on the measurements pins. For the low threshold value set at 100 MΩ, 78% nano coated SIR patterns and 63% acrylic coated SIR patterns measured above this value.

Table 5 contains a summary of the final measurements by board number and SIR pattern number: highlighted are the values that fall below the low threshold (100 MΩ), and bold font for values that meet and exceed the 5 GΩ value.

An additional graph (Figure 5) shows the summary of the test, and highlights the main effects based on averaging the relation between the surface treatment and the measured SIR values as compared to the 100 MΩ threshold value.

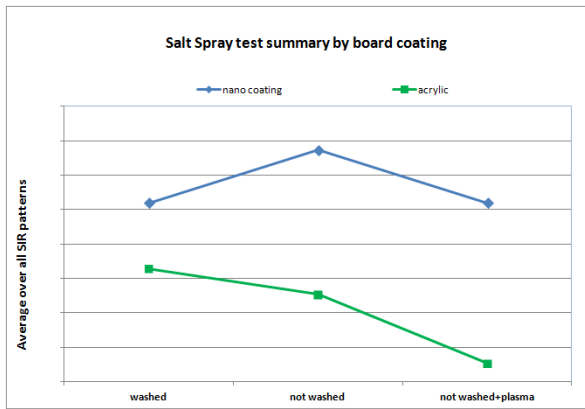


Figure 5. Salt spray test: Average ranking over all SIR patterns, irrespective of the geometry, for each surface treatment applied. Threshold limits 100 MΩ and 5 GΩ cannot be shown in the graph due to the numerous outliers (Table 5) and the smoothing effect introduced by the averaging process.

3. Humidity and Temperature Test.

The polarizing voltage of 5 VDC was disconnected prior to taking the required insulation resistance measurements. While in the chamber, the insulation resistance was measured and recorded at the following intervals: first, fourth, seventh, and tenth cycle. The measurements, during chamber exposure, were taken between hours 2 and 3 of the high temperature phase of each cycle specified.

After completion of the 160 hours, the bias voltage was disconnected and the specimens were removed from the chamber. The insulation resistance measurements were taken after an hour and before two hours at ambient laboratory conditions of 25°C with 40-50% relative humidity. The specimens were then stabilized for 24 hours at laboratory conditions of 25°C with 40-50% relative humidity prior to obtaining the final required insulation resistance measurements.

The plots of the measured SIR values are spaced out according to the time the samples spent in the chamber and the line connecting the values has the purpose to group data by board number, rather than being an interpolation of the intermediate values between measurements.

Each SIR pattern has a specific geometry. The data was grouped by the SIR pattern and by board type.

As can be seen from the plots, the acrylic coated boards show a more consistent behavior, with fewer instances of measurements below 100 MΩ than was observed for the nano coated boards.

This outcome contradicted the initial assumptions of the experiment that the nano conformal coating will outperform the traditional acrylic coating.

The lowest resistance values were shown by the boards that went through rework and recoating with the nano coating material.

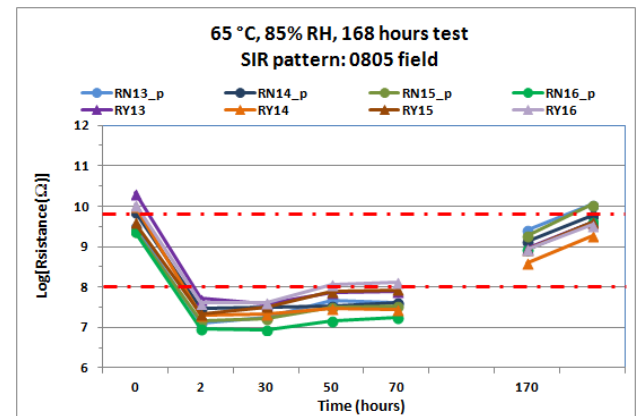
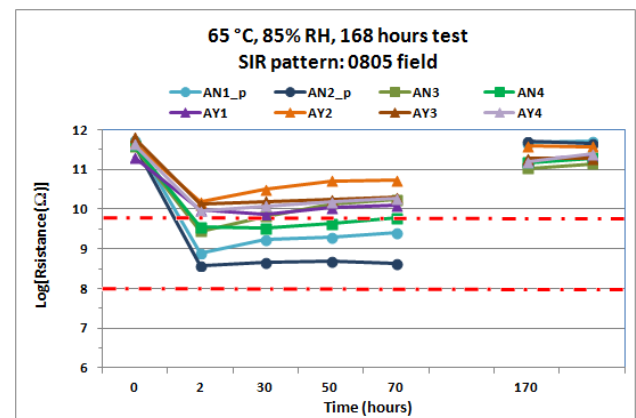
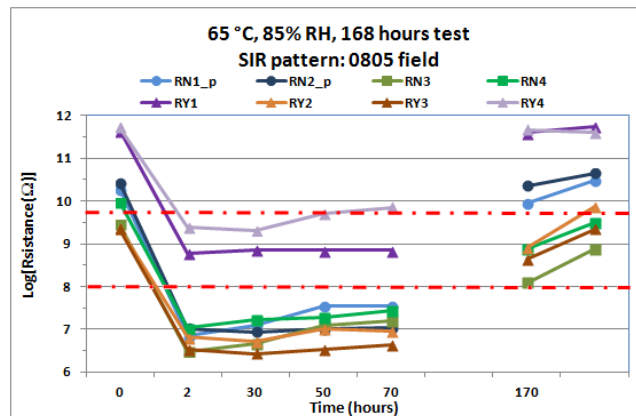


Figure 6. 0805 field. From top: nano coating – as applied; acrylic – as applied; nano coating – as reworked. (-p ≡ plasma treatment applied before coating)

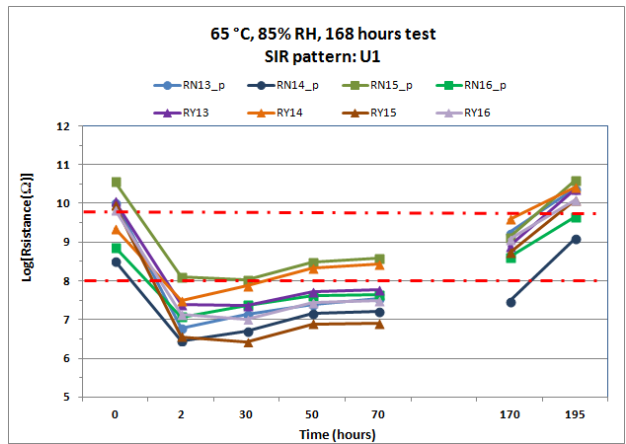
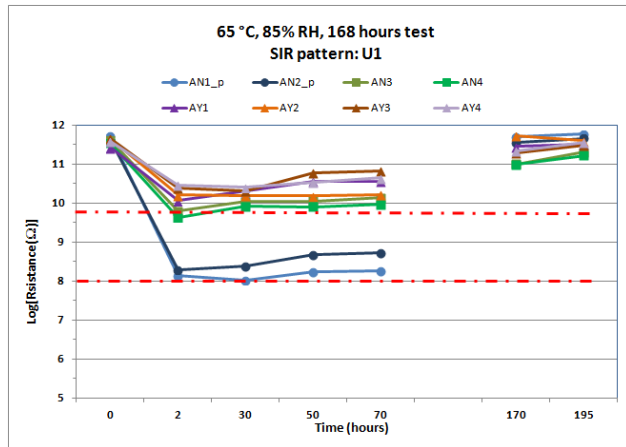
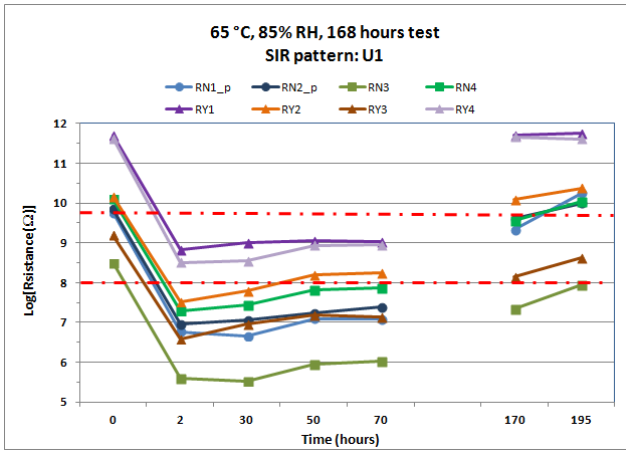


Figure 7. U1-BGA. From top: nano coating – as applied; acrylic – as applied; nano coating – as reworked. (-p ≡ plasma treatment applied before coating)

In summary, an average over the SIR patterns for each coating type and board treatment type yields the following semi quantitative result, which gives a visual representation of the influence of surface treatment on measured surface resistance values:

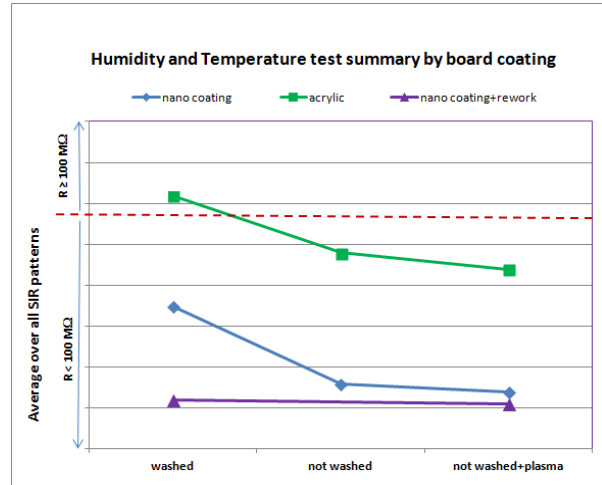


Figure 8. Temperature/humidity/bias (THB) test: Average ranking over all SIR patterns, irrespective of the geometry, for each surface treatment applied.

The dashed line in Figure 8 signifies the 100 MΩ threshold; the data points above the dashed line met the threshold condition 100% (all boards and all SIR patterns associated for the respective surface treatment case); only the acrylic coated, washed after SMT boards meet this condition 100%. After completion of all electrical testing, the test panels were examined for appearance. The summary of observations is included in Table 6.

The conformal coating was examined with 1.75X magnification with various light sources. Any referee inspection was carried out with 10X magnification. There was no evidence of peeling or blistering in the case of the acrylic coating. This is a considered an indication of good adhesion and board cleanliness, with expected low levels of ionic residue. During various tests both type coatings yielded lower SIR values for specific surface treatment conditions, although no dendrite growth was observed. This could indicate either the presence of trace ionic residue that is electrically active only after high levels of moisture are absorbed, or loss of integrity/reliability of the conformal coating material.

Table 6. Boards condition after THB test.

Temperature/Humidity/Bias (THB) Test		
Board label	Description	Observations after test
RN1, RN3	Nano coating, not washed after assembly	White film/residue on large portion of boards surface
RN13, RN14, RN15, RN16	Reworked boards; nano coating, not washed after assembly; plasma treated before coating.	White film/residue on large portion of boards surface
RY13, RY14, RY15, RY16	Reworked boards; nano coating, washed after assembly.	White film/residue on large portion of boards surface
RN2, RN4	Nano coating, not washed after assembly.	No anomalies observed
RY1, RY2, RY3, RY4	Nano coating, washed after assembly.	No anomalies observed
AN1, AN2, AN3, AN4	Acrylic coating, not washed after assembly.	No anomalies observed
AY1, AY2, AY3, AY4	Acrylic coating, washed after assembly.	No anomalies observed

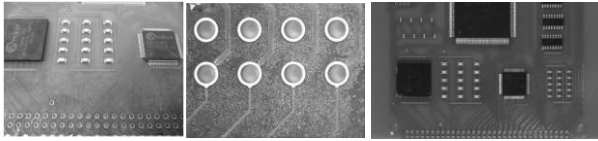


Figure 9. Example of white film/residue observed on some of the boards (nano coating) after humidity and temperature test (left and center). Acrylic coated board after THB testing (right).

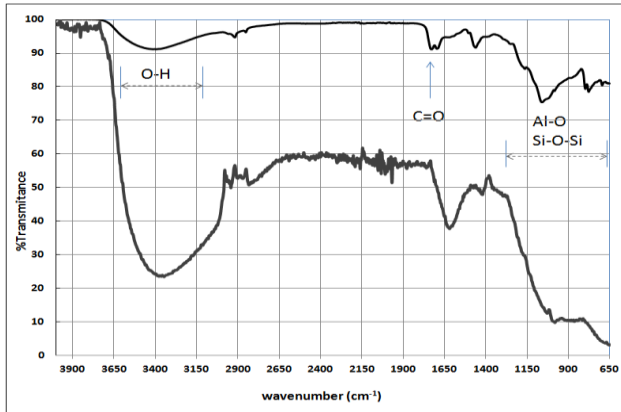
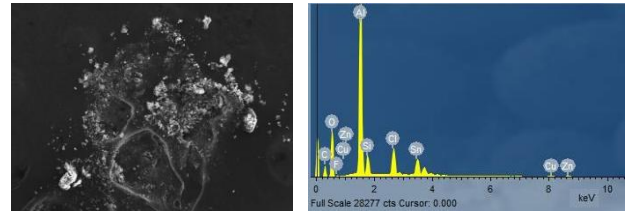


Figure 10. Top FTIR-ATR spectrum acquired on nano coated board with apparent white residue. Bottom FTIR-ATR spectrum of the harvested white substance (nanocoating material after exposure to THB test).

Elemental analysis via energy dispersive spectroscopy (EDS) and Fourier transform infrared spectroscopy (FTIR) has shown that the white appearance of the nano conformal coated boards could be an indication of the coarsening of the nano particles in the coating. A likeliest alternate hypothesis for the observations of the whitish aluminum oxide residues (after humidity and temperature test) is that it is due to a loss of fluorination of the film. The composition of the coated film was measured both while on the board and removed from the board using FTIR and SEM/EDS. The location of the elemental analysis is on an area of the board away from solder joints and any possibility of flux contamination at rework.

If an inactivated flux residue would have been left on the board, then the FTIR spectrum would be expected to show a strong peak at 1710 cm^{-1} corresponding to C=O bond [10] in any carboxylic acid.

For the FTIR spectrum taken on the board, the double peak seen at $\sim 1700\text{ cm}^{-1}$ is due to the signal collected from the solder mask under the nano coating film. Once the film is removed from the substrate, the double peak is not visible anymore. The functional groups that can be identified are O-H, Al-O and Si-O-Si, which are consistent to the expected nano coating composition.



	Weight%									
Sample	O	Al	C	Sn	Cl	Si	Cu	F	Zn	P
RN13	34.88	23.12	19.55	10.27	5.37	3.26	1.35	1.14	1.06	-
RY16	44.42	17.20	29.40	0.52	2.61	1.30	1.26	1.48	1.25	0.56

Figure 11. EDS analysis of white film residue collected from PCBA surface.

CONCLUSIONS

Physical properties of nano conformal coatings present them as an attractive alternative to the more traditional conformal coatings (acrylic, epoxy, and urethane). The current experiment was formulated to gather an initial set of measurements and side by side comparisons of test boards produced in the same conditions typical for lead free no clean SMT assembly.

Plasma treatment of the boards before application of the conformal coating had a positive influence only in the case of the corrosive gas testing. The plasma treated boards subjected to salt spray or temperature/humidity/bias testing did not show improved SIR values at the end of testing as compared to the not treated boards.

Washing the boards after SMT assembly did not influence the coating application or the SIR values for the corrosive gas or the salt spray test. Although it cannot be generalized, among the boards subjected to humidity and temperature testing, regardless of the coating type, the boards that measured close to the high threshold value were often from the batch that was washed after boards' assembly.

The SIR values were referenced to two different threshold values: $5\text{ G}\Omega$ / IPC-CC-830 and $100\text{ M}\Omega$ as is usually reported for humidity and temperature testing / IPC-9202. Reworked boards coated with acrylic were not included in the testing due to the size and scope of the experiment. Overall low SIR values measured on nano coated reworked boards during the humidity and temperature test are an indication of the possible influence of rework process. The 8 boards were reworked at selected locations (BGA, QFP, 1206 capacitors); all SIR patterns on the reworked nano coated boards measured lower than the equivalent patterns on the as assembled boards.

The acrylic coated boards presented the more consistent behavior for two of the tests, with the data running close together for groups of boards. Selected SIR patterns on some of the nano coated boards did show very promising values, however, repeatability was not accomplished in this

experimental run. More data is needed to identify the reason behind the low repeatability, as well as to why the reworked and recoated boards have shown the lowest SIR values at the end of humidity and temperature test.

The test for which nano coating outperformed the acrylic coating is the salt spray, where moisture was present as liquid water; on the THB test where moisture was in vapor form, the nano coating presented the least protection to the boards. Although acrylic coating performs better than the nano coating in two out of the three tests, it does not offer the desired level of protection in all harsh environmental testing conditions applied either.

It is preferable that the experiment be repeated in the future with a different nano coating material formulation, and include an additional conformal coating material (parylene – for example). As the nano coating material properties and application process evolve, it is desirable to compare its performance with the most used coatings as well as the better performing coatings (all other processes considered equal).

FUTURE WORK

A new nanocoating formulation film is available (since the completion of the experiment described here) for which an improved immobilization process is used. Instead of the silsesquioxane binding, a plasma polymerization of a siloxane is used. This results in improved thickness and binding of the nano-particles used for surface roughness. Additionally, this plasma process also facilitates an improved surface modification which can also be made thicker than the previous nanocoating film and upon further experimentation it is expected that this should improve the durability of the coating as well.

ACKNOWLEDGEMENTS

The authors gratefully acknowledge the management support of Marco Gonzalez from Sanmina, the material support and useful discussions of Ed Branco from Specialized Coating Services, and Sanmina Guadalajara process and management teams, especially of NPI team from Plant 1 and the support of the regional engineering team.

REFERENCES

- [1] Bin-Bin Wang, Jiang-Tao Feng, Ya-Pu Zhao, and T. X. Yu, *Journal of Adhesion Science and Technology* 24 (2010) 2693–2705.
- [2] J. Chinn, *Nanotech* 2010 Vol. 1, page 612 – 615.
- [3] Abidi, Nouredine, Luis Cabrales, and Payam Aminayi. "Molecular and Nanoparticles vapor deposition methods to create super-hydro/oleophobic surfaces." *Moroccan Journal of Chemistry* 3.1 (2014): Mor-J.
- [4] [foresiteinc.com:C3-Corrosivity-Index-12.15.14.pdf](#)
- [5] IPC-9203, 2012-May, Users Guide to IPC-9202 and the IPC-B-52 Standard Test Vehicle
- [6] IPC TM-650, method 2.6.3.4A.
- [7] Douglas Pauls, Courtney Slach, Nathan Devore, APEX® and the Designers Summit 2006.

[8] Fabio Stranges, Marianna Barberio, Pasquale Barone, Andrea Abenante, Andrea Leuzzi, Peppino Sapia, Fang Xu, Assunta Bonanno, *Archaeological Discovery* 2013. Vol.1, No.2, 32-36

[9] A. Mensah and C. Hunt, *The Role of Permeability and Ion Transport in Conformal Coating Protection*, NPL REPORT DEPC MPR 032, 2005

[10] Conseil, H., Jellesen, M. S., Verdingovas, V., & Ambat, R. (2013). Decomposition studies of no-clean solder flux systems in connection with corrosion reliability of electronics. In *EUROCORR 2013 - European Corrosion Congress*. [Paper H] European Federation of Corrosion.